

# New insight into the role of PTCH1 protein in serous ovarian carcinomas

VALENTINA KARIN-KUJUNDZIC<sup>1,2</sup>, ADRIANA COVARRUBIAS-PINTO<sup>3</sup>,  
ANITA SKRTIC<sup>2,4,5</sup>, SEMIR VRANIC<sup>6</sup> and LJILJANA SERMAN<sup>1,2</sup>

<sup>1</sup>Department of Biology and <sup>2</sup>Centre of Excellence in Reproductive and Regenerative Medicine, School of Medicine, University of Zagreb, 10000 Zagreb, Croatia; <sup>3</sup>Institute of Biochemistry II, School of Medicine, Goethe University, D-60590 Frankfurt am Main, Germany; <sup>4</sup>Department of Pathology, School of Medicine, University of Zagreb; <sup>5</sup>Department of Pathology, University Hospital Merkur, 10000 Zagreb, Croatia; <sup>6</sup>College of Medicine, QU Health, Qatar University, 2713 Doha, Qatar

Received February 23, 2022; Accepted August 18, 2022

DOI: 10.3892/ijo.2022.5435

**Abstract.** The Hedgehog (Hh) signaling pathway is essential for normal embryonic development, while its hyperactivation in the adult organism is associated with the development of various cancers. The role of the Hh signaling pathway in ovarian cancer has not been sufficiently investigated. Therefore, the present study investigated the role of protein patched homolog 1 (PTCH1), a component of the Hh signaling pathway, and changes in the promoter methylation status of the corresponding gene in a cohort of low-(LGSC) and high-grade serous ovarian carcinomas (HGSC) and HGSC cell lines (OVCAR8 and OVSAHO). PTCH1 protein expression level was analyzed using immunohistochemistry in tissue samples and immunofluorescence and western blotting in cell lines. DNA methylation patterns of the *PTCH1* gene were analyzed using methylation-specific PCR. PTCH1 protein expression was significantly higher in HGSCs and LGSCs compared with controls (healthy ovaries and fallopian tubes). Similarly, ovarian cancer cell lines exhibited significantly higher PTCH1 protein expression compared with a normal fallopian tube non-ciliated epithelial cell line (FNEI). PTCH1 protein fragments of different molecular weights were detected in all cell lines, indicating possible proteolytic cleavage of this protein, resulting in the generation of soluble N-terminal fragments that are translocated to the nucleus. DNA methylation of the *PTCH1* gene promoter was exclusively detected in a proportion of HGSC (13.5%) but did not correlate with protein expression. PTCH1 protein was highly expressed in serous ovarian

carcinoma tissues and cell lines, while *PTCH1* promoter methylation was only detected in HGSC. Further investigation is required to elucidate the possible mechanisms of PTCH1 activation in serous ovarian carcinomas.

## Introduction

Ovarian cancer is the eighth leading cause of cancer-associated mortality in females and is the third most common gynecological malignancy worldwide (1). This disease is a major clinical challenge in gynecological oncology, with the highest mortality rate of all malignancies of the female reproductive system (2). Most patients have almost no symptoms in the early stage of the disease. By contrast, nonspecific symptoms associated with more frequent benign conditions occur in the advanced stage of ovarian cancer, delaying the timely diagnosis of the disease (2,3). The diagnosis is further complicated because of different histological subtypes of ovarian cancer with various biological and clinical features (4).

Serous ovarian carcinomas are the most common form of ovarian cancer and account for a ~75% of all ovarian epithelial tumors. High-(HGSC) and low-grade serous ovarian carcinomas (LGSC) represent ~70% and <5% of all epithelial ovarian cancers, respectively (5). Although both are serous in histological type, HGSCs and LGSCs are two different entities with distinct pathogenesis, molecular and genetic changes, origin and prognosis (5). The exact origin of the LGSC and HGSC is still unknown. LGSC most likely arises from fallopian tube epithelium (FTE) (6), while the origin of HGSC is probably dual, and it may arise from ovarian surface epithelium (OSE) or FTE (7).

Aberrant activation of several signaling pathways, including the Hedgehog (Hh) signaling pathway, has been previously observed in ovarian cancer (8-10). The Hh signaling pathway is an evolutionarily conserved signaling pathway essential for the development of a normal embryo (11). However, in the adult organism, this signaling pathway is inactive in most organs, therefore its aberrant activation in adulthood is associated with the development of various cancer types, such

---

*Correspondence to:* Dr Valentina Karin-Kujundzic, Department of Biology, School of Medicine, University of Zagreb, Salata 3, 10000 Zagreb, Croatia  
E-mail: valentina.karin@mef.hr

**Key words:** ovarian cancer, serous ovarian carcinoma, ovarian cancer cell lines, Hedgehog signaling pathway, protein patched homolog 1

as skin, brain, liver, gallbladder, pancreas, stomach, colon, breast, lung and prostate cancer, as well as hematological malignancies (11,12).

The Hh signaling pathway is activated when one of the three Hh ligands, sonic hedgehog, indian hedgehog or desert hedgehog, binds to 12-pass transmembrane receptor protein patched homolog 1 (PTCH1) or protein patched homolog 2 (PTCH2), thus suppressing its activity. In the absence of Hh ligands, activated PTCH1 represses Hh signaling (13,14). PTCH1 is the primary receptor of the Hh signaling pathway. The human *PTCH1* gene encodes a transmembrane glycoprotein of 1,447 amino acids (~161 kDa) (15). PTCH1 receptor contains a transmembrane domain, two large extracellular domains (ECDs), ECD1 and ECD2 and three large cytoplasmic domains, N-terminal domain (NTD), middle loop and C-terminal domain (16,17).

Although PTCH1 is a negative regulator of Hh signaling, this receptor serves as a marker of canonical Hh signaling activation (18). Since the *PTCH1* gene contains binding sites for GLI transcription factors, its expression is enhanced when Hh signaling is activated, creating a negative feedback loop (19,20). If PTCH1 loses its function, either due to gene mutations or epimutations, aberrant activation of the Hh signaling will occur (12). Inactivating mutations and hypermethylation of the *PTCH1* gene have been observed in various cancer types, such as colorectal, breast, gastric, ovarian and basal cell carcinoma (21-27). However, numerous studies have shown that PTCH1 protein, otherwise known to act as a tumor suppressor, has increased expression in several cancers, including breast, prostate, lung, colon, brain cancers and melanoma (28-30). A recent study has shown that the PTCH1 receptor can also serve as a transporter that releases chemotherapeutic agents out of the cell and thus contributes to chemotherapy resistance (30). The increased expression of PTCH1 protein in the tumor tissue can be attributed to possible changes in the structure and function of this protein during carcinogenesis. These changes can be triggered by mutations in the *PTCH1* gene, whereby PTCH1 loses its original tumor suppressor role and gains a novel tumor promoter role (22).

Increased expression of the PTCH protein has also been observed in ovarian cancer, where expression of this protein was increased stepwise in benign, borderline and malignant neoplasms (31). PTCH protein expression was associated with increased tumor cell proliferation and was positively correlated with poor survival of patients with ovarian cancer (31,32). On the other hand, there are studies with conflicting results where reduced expression of PTCH1 protein has been observed in ovarian tumor tissues and ovarian cancer cell lines (33,34). Patients with ovarian cancer with decreased expression of PTCH1 protein were found to have a poorer prognosis than patients with increased expression of this protein (34).

Although the aforementioned studies have shown that PTCH1 could be involved in the molecular pathogenesis of ovarian cancer, its role in ovarian cancer subtypes has not been sufficiently investigated. Therefore, the present study further explored the role of PTCH1 protein and its promoter methylation status in serous ovarian carcinomas and corresponding cell lines.

## Materials and methods

**Tissue samples.** Formalin-fixed paraffin-embedded (FFPE) samples of 48 serous ovarian carcinomas (LGSC, n=11; HGSC, n=37), 20 samples of healthy ovarian tissue and 10 samples of healthy fallopian tube tissue were used for the present study. Other histologic subtypes of invasive ovarian carcinomas (e.g., mucinous, endometrioid or clear cell carcinomas), borderline and benign tumors were excluded from the study. The age ranges were as follows: 37-81 years for the HGSC group, 48-86 years for the LGSC group, 52-81 years for the healthy ovarian control group and 50-68 years for the fallopian tube control group; there were no significant differences among the groups in terms of age. Board-certified pathologists reviewed the representative slides (SV and AS) to confirm the diagnosis (LGSC or HGSC) and selected appropriate healthy and malignant tissues for immunohistochemical and molecular analyses. Both pathologists were completely blinded to the clinical and pathological information of the subjects. They assessed the samples independently and in case of any discrepancy, a consensus was reached using a double-headed microscope. The tissue samples used in the current study were a part of the archival collection of cancer tissue samples, collected from January 2000 to January 2012, from the School of Medicine, University of Zagreb, assembled in collaboration with University Hospital Merkur, both of which are part of the Scientific Center of Excellence in Reproductive and Regenerative Medicine (Zagreb, Croatia).

**Cell lines and culture.** HGSC cell lines, OVCAR8 and OVSAHO, and normal telomerase reverse transcriptase-immortalized fallopian tube non-ciliated epithelial cell line FNE1 (serving as normal control) were used in the current study. OVCAR8 was a kind gift from Dr Ernst Lengyel (University of Chicago). OVSAHO was obtained from the Japanese Collection of Research Bioresources Cell Bank and FNE1 from the Live Tumor Culture Core (University of Miami, Sylvester Comprehensive Cancer Center). OVCAR8 and OVSAHO cell lines were grown in DMEM with 4.5 g/l D-glucose and L-glutamine (Gibco; Thermo Fisher Scientific, Inc.) along with 10% FBS (Gibco; Thermo Fisher Scientific, Inc.), 1 mM sodium pyruvate (Sigma-Aldrich; Merck KGaA), 1% MEM vitamins (Gibco; Thermo Fisher Scientific, Inc.), 1% MEM nonessential amino acids (Sigma-Aldrich; Merck KGaA) and 1% penicillin-streptomycin (Sigma-Aldrich; Merck KGaA). FNE1 cells were grown in Fallopian Ovary Modified Ince medium (Live Tumor Culture Core, University of Miami, Sylvester Comprehensive Cancer Center) supplemented with 25 ng/ml cholera toxin (Sigma-Aldrich; Merck KGaA) in Corning® Primaria™ cell culture dishes (Corning, Inc.). All cell lines were cultured at 37°C in a humidified atmosphere with 5% CO<sub>2</sub>.

**Immunohistochemistry (IHC).** IHC staining was performed using the biotin-avidin-streptavidin HRP method with the Dako REAL Envision detection system; cat. no. K0679; Dako; Agilent Technologies, Inc.) used for visualization according to the manufacturer's instructions on 4- $\mu$ m thick FFPE sections that were placed on silanized glass slides (Dako; Agilent Technologies, Inc.) as previously described (35). The sections

were counterstained with hematoxylin at room temperature (RT) for 1 min. The primary antibodies (anti-PTCH1) used in this experiment are listed in Table I. Healthy placental tissue (part of a collection of placental tissue samples, collected from January 2012 to December 2012, belonging to the University of Zagreb School of Medicine that had been collected in collaboration with the University Hospital Merkur, both of which are parts of the Scientific Center of Excellence for Reproductive and Regenerative Medicine) was used as a positive control (data not shown). The negative control was treated similarly with the omission of incubation with the primary antibodies. Tissue sections were examined using a light microscope (Olympus CX22; Olympus Life Science).

PTCH1 expression in serous ovarian carcinomas and healthy tissues was interpreted independently by two pathologists (SV and AS). The quantification was performed using the H-score system. The intensity, scored between no staining (0) and strong staining (3+), and the proportion of the PTCH1 protein in different cellular compartments (cytoplasm and nucleus) were assessed. The score was obtained using the following formula: H-score = (% of weakly stained cytoplasm/nuclei x1) + (% of moderately stained cytoplasm/nuclei x2) + (% of strongly stained cytoplasm/nuclei x3). The range of possible scores was between 0 and 300. PTCH1 protein expression was observed in epithelial and stromal cells. H-score for total expression of PTCH1 protein was calculated as a sum of H-scores obtained for the cytoplasmic and nuclear protein expression, with the range of possible scores between 0 and 600. In case of discordant interpretation, the pathologists reviewed cases together to obtain a complete concordance. Few samples of HGSC and LGSC tissues were stained for PTCH1 protein using anti-PTCH1b, anti-PTCH1c, and anti-PTCH1d antibodies to confirm the subcellular localization of PTCH1 protein.

**Immunofluorescence (IF).** Cells (OVCAR8, OVSAHO and FNE1) grown on glass coverslips (Thermo Fisher Scientific, Inc.) were fixed with 4% paraformaldehyde solution (Santa Cruz Biotechnology, Inc.) for 15 min at RT. Samples were washed with 1X DPBS buffer (Gibco; Thermo Fisher Scientific, Inc.) and permeabilized with 0.1% saponin (Sigma-Aldrich; Merck KGaA) in 1X DPBS (PMS buffer) for 10 min at RT. After permeabilization, cells were incubated in blocking buffer (PMS buffer with 5% FBS) for 1 h at RT. Samples were incubated overnight at 4°C with primary anti-PTCH1 antibodies listed in Table I. All anti-PTCH1 antibodies were used for IF staining. Cells were washed and incubated for 1 h at RT with solution containing anti-rabbit Alexa Fluor 488 (dilution 1:300; cat. no. A-21206; Invitrogen; Thermo Fisher Scientific, Inc.) or anti-mouse Cy3 antibody (dilution 1:300; cat. no. 715-165-150; Jackson ImmunoResearch Europe, Ltd.) with Hoechst 33342 stain (NucBlue Live ReadyProbes Reagent; dilution 1:10; Invitrogen; Thermo Fisher Scientific, Inc.). After incubation with secondary antibodies, samples were washed and mounted using a fluorescence mounting medium (Dako; Agilent Technologies, Inc.). Cells were examined using an inverted Leica SP8-X FLIM confocal microscope. ImageJ software version 1.51 (function 'measure'; National Institutes of Health) was used to quantify mean fluorescence intensity.

**Western blot analysis.** Total proteins were isolated from OVCAR8, OVSAHO, and FNE1 cell lines using ice-cold RIPA buffer (150 mM NaCl, 50 mM Tris/HCl pH 8.0, 1% Triton X-100, 0.5% sodium deoxycholate, 0.1% SDS) containing complete protease inhibitor (Roche Diagnostics) and 1 mM PMSF (Thermo Fisher Scientific, Inc.) as previously described (36). Protein concentrations were determined by the BCA assay (Sigma-Aldrich; Merck KGaA) according to the manufacturer's instructions. The Subcellular Protein Fractionation Kit for Cultured Cells (cat. no. 78840; Thermo Fisher Scientific, Inc.) was used to segregate and enrich proteins from five cellular compartments (cytoplasmic, membrane, nuclear soluble, chromatin-bound and cytoskeletal proteins). Proteins were enriched and extracted according to the manufacturer's instructions.

For western blot analysis, 10% polyacrylamide gels were used to separate 10 µg of total protein samples/lane and 10 µl of each protein fraction. Western blotting was performed as previously described (36). The membranes were probed with rabbit polyclonal anti-GAPDH antibody (dilution, 1:2,000; cat. no. IMG-5143A; IMGENEX), rabbit monoclonal anti-Na<sup>+</sup>/K<sup>+</sup> ATPase antibody (dilution, 1:50,000; cat. no. ab76020; Abcam), goat polyclonal anti-fibrillarin antibody (dilution, 1:1,000; cat. no. sc-11335; Santa Cruz Biotechnology, Inc.), mouse monoclonal anti-H3K4me2 antibody (dilution, 1:2,000; clone CMA303; cat. no. 05-1338; Sigma-Aldrich; Merck KGaA) and rabbit polyclonal anti-β-actin antibody (dilution, 1:2,000; cat. no. ab8227; Abcam) to verify the efficiency of protein extraction from different cellular compartments. Anti-PTCH1 primary antibodies used in this experiment are listed in Table I. HRP-conjugated secondary antibodies goat anti-rabbit (dilution, 1:5,000; cat. no. P0448; Dako; Agilent Technologies, Inc.), donkey anti-goat (dilution, 1:10,000; cat. no. sc-2033; Santa Cruz Biotechnology, Inc.), goat anti-mouse (dilution, 1:12,500; cat. no. 170-6516; Bio-Rad Laboratories, Inc.) and SuperSignal™ West Femto Maximum Sensitivity Substrate (Thermo Fisher Scientific, Inc.) were used to visualize reactive bands.

**Methylation-specific PCR.** DNA was isolated from two 10-µm sections of FFPE tissue as previously described (37). DNA was also extracted from cultured cells (OVCAR8, OVSAHO and FNE1) using cell lysis buffer (100 mM NaCl, 10 mM Tris pH 8.0, 25 mM EDTA pH 8.0, 0.5% SDS, 0.1 mg/ml proteinase K; 1 ml buffer per 10<sup>8</sup> cells). Samples were incubated in lysis buffer overnight at 300 revolutions/min and 50°C. An equal volume of ROTI®Phenol/Chloroform/Isoamyl alcohol (Carl Roth GmbH & Co. Kg) was added to the lysed cell suspensions. Samples were vortexed vigorously and subsequently centrifuged at 16,000 x g for 5 min at RT. The aqueous phase containing the purified DNA was transferred to a clean tube. DNA was precipitated using ice-cold absolute ethanol. Isolated DNA was treated with bisulfite using the MethylEdge Bisulfite Conversion System (Promega Corporation) according to the manufacturer's instructions. Bisulfite-treated DNA was used for the methylation-specific PCR. Primers for *PTCH1* promoter region were synthesized according to Peng *et al* (38): Methylated *PTCH1* forward, 5'-AATTAAGGAGTTGTTGCGGTC-3' and reverse, 5'-GCTAAACCATTCTATCCCCGTA-3' (125 bp); unmethylated *PTCH1* forward, 5'-ATTAAGGAGTTGTTGTGGTTGT-3' and

reverse, 5'-ACTAAACCATTCTATCCCCATA-3' (124 bp). All PCRs were performed using TaKaRa EpiTaq HS (for bisulfite-treated DNA) (Takara Bio, Inc.), including 1X EpiTaq PCR Buffer (Mg<sup>2+</sup> free), 2.5 mM MgCl<sub>2</sub>, 0.3 mM dNTPs, 20 pmol of each primer (Sigma-Aldrich; Merck KGaA), 50 ng DNA and 1.5 unit TaKaRa EpiTaq HS DNA Polymerase in a 50  $\mu$ l final reaction volume. PCR cycling conditions for both unmethylated and methylated primers were as follows: Initial denaturation at 95°C for 30 sec, followed by 40 cycles of 95°C for 30 sec, 61°C for 30 sec and 72°C for 30 sec, followed by a final extension at 72°C for 7 min. PCR products were separated on 2% agarose gels, stained with GelStar Nucleic Acid Gel Stain (Lonza Group, Ltd.) and visualized on a UV transilluminator. Methylated Human Control DNA (Promega Corporation) was used as a positive control for the methylated reaction, unmethylated human EpiTect Control DNA (Qiagen GmbH) was used as a positive control for the unmethylated reaction, and nuclease-free water was used as a negative control.

**Statistical analysis.** The Kolmogorov-Smirnov and Shapiro-Wilk W tests were employed to assess the distribution of the data. SPSS software v21 (IBM Corp.) was used for the statistical analysis. The difference in total, cytoplasmic and nuclear expression of PTCH1 protein among ovarian tumor samples compared with healthy ovarian and fallopian tube tissue was assessed using Kruskal-Wallis followed by Dunn's multiple comparisons test, while the difference in the expression of PTCH1 between the epithelium and stroma of ovarian tumor samples and normal tissue samples was assessed using the Wilcoxon signed-rank test. Spearman's correlation was used to examine the correlation between DNA promoter methylation of the *PTCH1* gene and the expression of the corresponding protein. The difference in mean fluorescence intensity among cancer (OVCAR8 and OVSAGO) and control (FNE1) cell lines was assessed using Kruskal-Wallis followed by Dunn's multiple comparisons test. The IF experiment was repeated three times for each cell line.  $P < 0.05$  was considered to indicate a statistically significant difference.

## Results

***PTCH1* protein expression in serous ovarian carcinomas.** Analysis of PTCH1 protein expression indicated increased nuclear expression of this protein in tumor tissues (Fig. 1A and B). In addition to nuclear expression, cytoplasmic expression of this protein was also observed (Fig. 1A-D). The results of IHC analysis of nuclear, cytoplasmic and total PTCH1 protein expression in tumor epithelium and its connective stroma and epithelial and stromal compartments of control samples are shown in Fig. 1E-J.

**Total expression of *PTCH1* protein.** PTCH1 protein expression was significantly higher in the tumor epithelium of HGSCs and LGSCs compared with healthy OSE ( $P < 0.0001$  and  $P = 0.001$ , respectively) and in the tumor epithelium of HGSCs and LGSCs compared with FTE ( $P = 0.026$  and  $P = 0.038$ , respectively) (Fig. 1E). There was no statistically significant difference in PTCH1 protein expression in tumor epithelium between HGSCs and LGSCs ( $P = 1.000$ ), nor in healthy

epithelium between ovaries and fallopian tubes ( $P = 1.000$ ) (Fig. 1E).

In the connective stroma, PTCH1 protein expression was significantly higher in healthy ovaries compared with healthy fallopian tubes ( $P = 0.019$ ). However, there was no statistically significant difference in the expression of this protein in the connective stroma of HGSCs and LGSCs compared with healthy ovarian ( $P = 1.000$  and  $P = 1.000$ , respectively) and fallopian tube stroma ( $P = 0.073$  and  $P = 0.060$ , respectively), as well as between HGSCs and LGSCs ( $P = 1.000$ ) (Fig. 1F).

In contrast to healthy fallopian tubes ( $P = 0.139$ ), PTCH1 protein expression was significantly higher in the tumor epithelium compared with the connective stroma of HGSCs ( $P < 0.0001$ ) and LGSCs ( $P = 0.013$ ), as well as in stromal compared with epithelial tissue of normal ovaries ( $P = 0.012$ ).

**Cytoplasmic expression of *PTCH1* protein.** There was no statistically significant difference in the cytoplasmic expression of PTCH1 protein in the tumor epithelium of HGSCs and LGSCs compared with healthy OSE and FTE, between the tumor epithelium of HGSCs and LGSCs, as well as between OSE and FTE (Fig. 1G).

In the stromal compartment, the cytoplasmic expression of PTCH1 protein was significantly higher in healthy ovaries compared with healthy fallopian tubes ( $P = 0.015$ ). At the same time, there was no statistically significant difference in the cytoplasmic expression of this protein in the connective stroma of HGSCs and LGSCs compared with healthy ovarian ( $P = 1.000$  and  $P = 1.000$ , respectively) and fallopian tube stroma ( $P = 0.123$  and  $P = 0.425$ , respectively), as well as between the connective stroma of HGSCs and LGSCs ( $P = 1.000$ ) (Fig. 1H).

Cytoplasmic expression of PTCH1 protein was not significantly different between tumor epithelial tissue and connective stroma in HGSCs ( $P = 0.474$ ) and LGSCs ( $P = 0.110$ ), nor between epithelial and stromal tissue in healthy ovaries ( $P = 0.218$ ) and fallopian tubes ( $P = 0.268$ ).

**Nuclear expression of *PTCH1* protein.** Nuclear expression of PTCH1 protein was significantly higher in the tumor epithelium of HGSCs and LGSCs compared with healthy OSE ( $P < 0.0001$  and  $P < 0.0001$ , respectively) and in the tumor epithelium of HGSCs compared with healthy FTE ( $P = 0.020$ ) (Fig. 1I). There was no statistically significant difference in the nuclear expression of PTCH1 protein in the tumor epithelium of LGSCs compared with healthy FTE ( $P = 0.151$ ), in the tumor epithelium between HGSCs and LGSCs ( $P = 1.000$ ), as well as between healthy OSE and FTE ( $P = 0.254$ ) (Fig. 1I).

In the stromal compartment, there was no statistically significant difference in the nuclear expression of PTCH1 protein in HGSCs and LGSCs compared with healthy ovaries and fallopian tubes, between HGSCs and LGSCs, as well as between healthy ovaries and fallopian tubes (Fig. 1J).

Nuclear expression of PTCH1 protein was significantly higher in the tumor epithelium than in the connective stroma of HGSCs ( $P < 0.0001$ ) and LGSCs ( $P = 0.016$ ), as well as in the epithelium of healthy fallopian tubes compared with their stroma ( $P = 0.040$ ). By contrast, in healthy ovaries, nuclear expression was significantly higher in stromal than in epithelial tissue ( $P < 0.0001$ ).

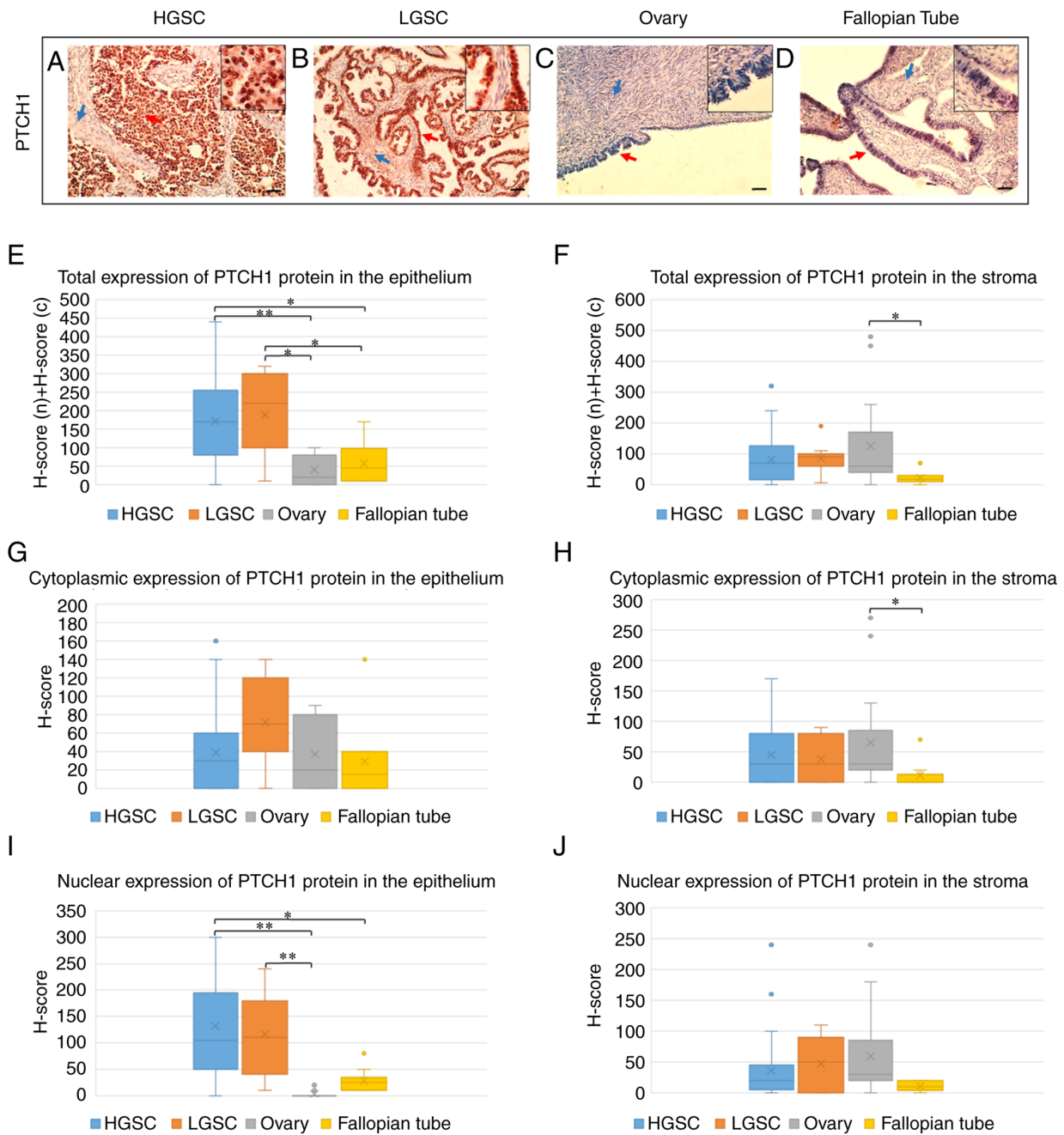


Figure 1. Immunohistochemical staining of PTCH1 protein in (A) HGSC, (B) LGSC, (C) healthy ovarian tissue and (D) healthy fallopian tube tissue. Red arrows point to the epithelium, while blue arrows point to the stroma (scale bar, 100  $\mu$ m; magnified windows, magnification, x400). (E) Total, (G) cytoplasmic and (I) nuclear expression of PTCH1 protein in the tumor epithelium of HGSCs and LGSCs and epithelium of healthy ovaries and fallopian tubes, and (F) total, (H) cytoplasmic and (J) nuclear expression of PTCH1 protein in the connective stroma of HGSCs and LGSCs and ovarian and fallopian tube stroma, determined by immunohistochemical analysis (H-score). H score (n) + H score (c) is a sum of H-scores calculated for the nuclear and cytoplasmic protein expression. \* $P < 0.05$ , \*\* $P < 0.0001$ . HGSC, high-grade serous ovarian carcinoma; LGSC, low-grade serous ovarian carcinoma; PTCH1, protein patched homolog 1; n, nuclear; c, cytoplasmic.

IHC confirmed nuclear localization of PTCH1 protein in HGSC and LGSC tissue samples using four different anti-PTCH1 antibodies: Anti-PTCH1a, anti-PTCH1b, anti-PTCH1c, and anti-PTCH1d (Table I and Fig. S1). In addition to nuclear staining, cytoplasmic localization of this protein was observed with all four antibodies. In samples treated with anti-PTCH1d antibody, PTCH1 protein was strongly expressed in the cytoplasm, while its nuclear expression was weaker than in samples treated with anti-PTCH1a, anti-PTCH1b, and anti-PTCH1c antibodies (Fig. S1).

*PTCH1 protein expression in HGSC cell lines.* Since nuclear localization of PTCH1 protein has not been reported in ovarian cancers, PTCH1 expression and subcellular localization was further investigated using IF analysis in HGSC cell lines. In OVCAR8, OVSAHO, and FNE1 cell lines, PTCH1 protein expression was detected using two different antibodies, anti-PTCH1a and anti-PTCH1d (Table I). PTCH1 protein detected using the anti-PTCH1a antibody was mainly localized in the nucleus in both cancer cell lines. In this case, PTCH1 protein expression was significantly higher in the

Table I. List and specifications of anti-PTCH1 primary antibodies used in IHC, IF and WB.

Antibody	Antigen	Host and clonality	Epitope, aa	Dilution	Catalogue number and manufacturer
Anti-PTCH1a	PTCH1	Rabbit polyclonal	1-50	IHC, 1:500; IF, 1:100; WB, 1:1,000	ab129341; Abcam
Anti-PTCH1b	PTCH1	Rabbit polyclonal	1-50	IHC, 1:300; IF, 1:100; WB, 1:1,000	ab53715; Abcam
Anti-PTCH1c	PTCH1	Rabbit polyclonal	1-80	IHC, 1:300; IF, 1:100; WB, 1:1,000	OASG05688; Aviva Systems Biology, Corp.
Anti-PTCH1d	PTCH1	Mouse monoclonal	122-436	IHC, 1:50; IF, 1:25; WB, 1:500	NBP1-47945; Novus Biologicals, LLC

IHC, immunohistochemistry; IF, immunofluorescence; WB, western blotting; aa, amino acid; PTCH1, protein patched homolog 1.

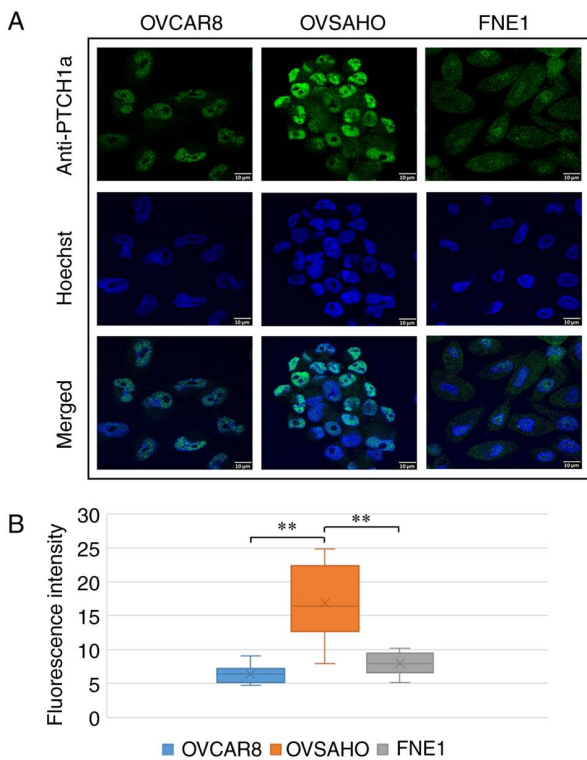


Figure 2. Immunofluorescence staining of PTCH1 protein in high-grade serous ovarian carcinoma cell lines, OVCAR8 and OVSAHO, and normal fallopian tube non-ciliated epithelial cell line FNE1. (A, first row) Staining with an anti-PTCH1a antibody. (A, second row) Nuclei stained with Hoechst. (A, third row) Merged images (scale bars, 10  $\mu$ m). (B) Mean fluorescence intensity of PTCH1 protein in OVCAR8, OVSAHO and FNE1 cell lines. \*\* $P<0.0001$ . PTCH1, protein patched homolog 1.

OVSAHO cell line compared with the OVCAR8 cell line ( $P<0.0001$ ) and control cell line FNE1 ( $P<0.0001$ ) (Fig. 2). In contrast to the anti-PTCH1a antibody, PTCH1 protein detected by the anti-PTCH1d antibody was primarily localized in the cytoplasm in cancer cell lines, while PTCH1 protein expression was significantly higher in both OVCAR8 and OVSAHO cancer cell lines compared with the control cell line ( $P=0.006$  and  $P<0.0001$ , respectively), as well as in OVSAHO compared with OVCAR8 cancer cell line ( $P=0.047$ ) (Fig. 3).

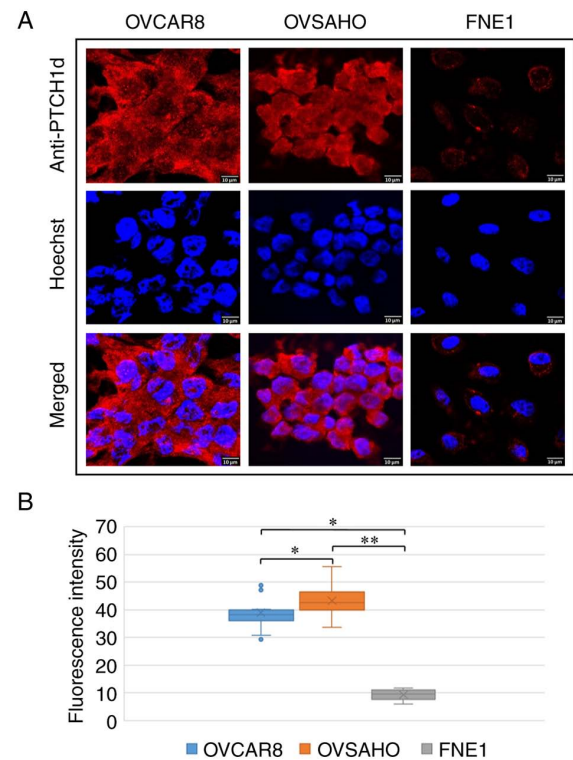


Figure 3. Immunofluorescence staining of PTCH1 protein in high-grade serous ovarian carcinoma cell lines, OVCAR8 and OVSAHO, and normal fallopian tube non-ciliated epithelial cell line FNE1. (A, first row) Staining with an anti-PTCH1d antibody. (A, second row) Nuclei stained with Hoechst. (A, third row) Merged images (scale bars, 10  $\mu$ m). (B) Mean fluorescence intensity of PTCH1 protein in OVCAR8, OVSAHO and FNE1 cell lines. \* $P<0.05$ , \*\* $P<0.0001$ . PTCH1, protein patched homolog 1.

PTCH1 protein expression in cell lines was also detected using the anti-PTCH1b and anti-PTCH1c antibodies (Table I). PTCH1 was predominantly localized in the nucleus in both cancer cell lines, and its expression was higher in cancer than in the control cell line ( $P<0.0001$  for all statistical calculations) (Figs. S2 and S3). When looking at the cytoplasm, there were punctate signals observed in this cellular compartment in the case of all four anti-PTCH1 antibodies (Figs. 2, 3, S2 and S3).

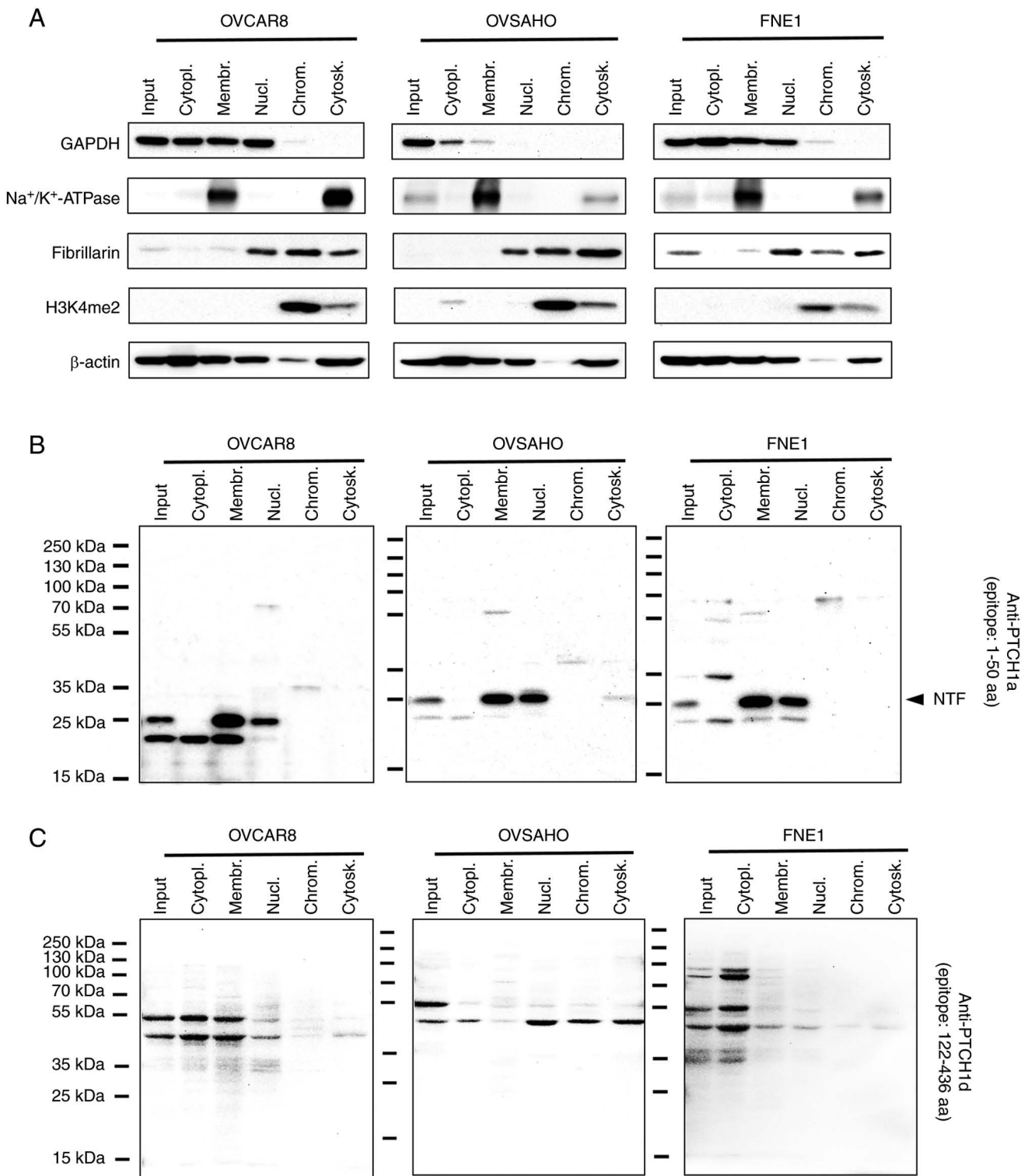


Figure 4. Subcellular localization of PTCH1 protein in high-grade serous ovarian carcinoma cell lines, OVCAR8 and OVSAHO, and normal fallopian tube non-ciliated epithelial cell line FNE1. (A) Efficiency of protein extraction from different cellular compartments was verified by examining the expression of GAPDH protein in the cytoplasmic protein fraction, Na<sup>+</sup>/K<sup>+</sup> ATPase in the membrane fraction, fibrillarin in the nuclear soluble protein fraction, H3K4me2 protein in the chromatin-bound protein fraction and β-actin in the cytoskeletal protein fraction. Western blotting using (B) anti-PTCH1a and (C) anti-PTCH1d antibodies. PTCH1, protein patched homolog 1; input, total proteins; cytopl., cytoplasmic proteins; membr., membrane proteins; nucl., nuclear soluble proteins; chrom., chromatin-bound proteins; cytosk., cytoskeletal proteins; NTF; N-terminal cytoplasmic fragment; aa, amino acids.

*Subcellular localization of PTCH1 protein in HGSC cell lines.* Subcellular localization of PTCH1 protein in OVCAR8, OVSAHO, and FNE1 cell lines was analyzed by western blotting. The expression of PTCH1 protein in different cellular

compartments (cytoplasmic, membrane, nuclear soluble, chromatin-bound and cytoskeletal) was detected using two different antibodies, anti-PTCH1a and anti-PTCH1d (Table I). The efficiency of protein isolation from different cellular

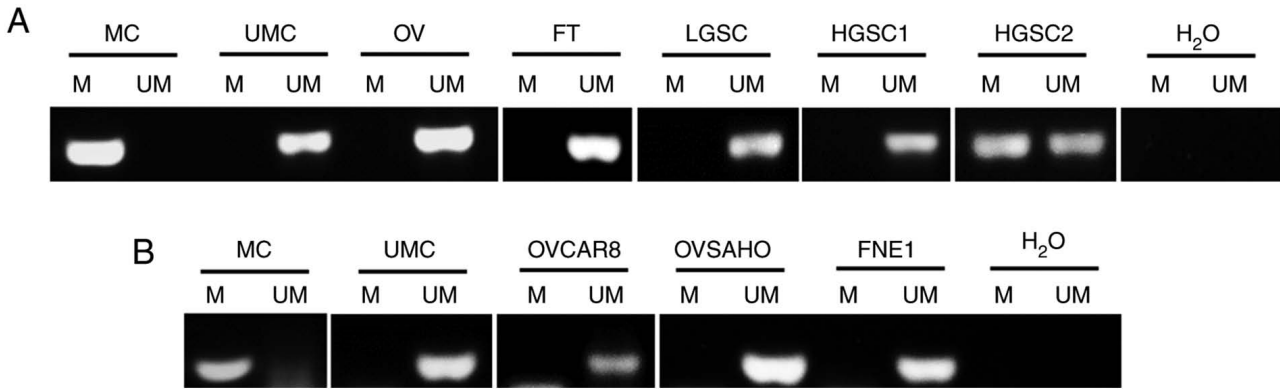


Figure 5. Methylation-specific PCR analysis of the *PTCH1* gene in serous ovarian carcinomas and ovarian cancer cell lines. (A) Representative images of methylation-specific PCR analysis for *PTCH1* gene promoter in healthy OV and FT tissues, LGSC and HGSC. (B) DNA promoter methylation status of the *PTCH1* gene in HGSC cell lines, OVCAR8 and OVSAHO, and normal fallopian tube non-ciliated epithelial cell line FNE1. M, methylated reaction; UM, unmethylated reaction; MC, methylated human control; UMC, unmethylated human control; OV, ovarian; FT, fallopian tube; HGSC, high-grade serous ovarian carcinoma; LGSC, low-grade serous ovarian carcinoma.

compartments was analyzed by checking the presence of GAPDH protein in the cytoplasmic protein fraction, Na<sup>+</sup>/K<sup>+</sup> ATPase in the membrane fraction, fibrillarin in the nuclear soluble protein fraction, H3K4me2 protein in the chromatin-bound protein fraction and  $\beta$ -actin in the cytoskeletal protein fraction (Fig. 4A). In addition to the cytoskeletal fraction,  $\beta$ -actin may also be found in the cytoplasmic, membrane and nuclear protein fractions (39,40). Since extracts from each subcellular compartment generally have <15% contamination between fractions (that is why it is considered an enriched fraction of each compartment according to the manufacturer, which is sufficient purity for most experiments studying protein localization and redistribution), this protein may appear in different protein fractions. Analysis of total proteins confirmed the presence of PTCH1 protein in all cell lines using both antibodies (Fig. 4B and C).

PTCH1 protein detected by the anti-PTCH1a antibody was primarily present in the membrane and nuclear soluble protein fractions (Fig. 4B). By contrast, when anti-PTCH1d antibody was used, this protein was mainly present in the cytoplasmic fraction (with the exception of the OVSAHO cell line) (Fig. 4C). PTCH1 protein expression in different cellular compartments was also detected using anti-PTCH1b and anti-PTCH1c antibodies. PTCH1 protein was primarily present in membrane and nuclear soluble fractions (Fig. S4), as in the case of the anti-PTCH1a antibody. In all four cases, fragments of PTCH1 protein of different molecular weights were detected, which indicates the possibility of proteolytic cleavage of this protein (Figs. 4B and C and S4).

**DNA promoter methylation of the *PTCH1* gene in serous ovarian carcinomas.** DNA promoter methylation of *PTCH1* was exclusively observed in HGSCs (5/37 cases, 13.5%), while no methylation was detected in any LGSCs and healthy ovarian and fallopian tube tissues (Fig. 5A). There was no correlation between DNA promoter methylation of the *PTCH1* gene and total expression of PTCH1 protein in HGSCs (analyzed in the whole tissue sections) ( $\rho=0.122$ ;  $P=0.470$ ). The *PTCH1* gene promoter was unmethylated in OVCAR8, OVSAHO, and FNE1 cell lines (Fig. 5B).

## Discussion

Aberrant expression of PTCH1 protein has been reported in various cancer types, such as lung, breast, prostate, ovary, colon and brain cancer, as well as melanoma (28-32). To the best of our knowledge, this is the first study reporting a high nuclear expression of PTCH1 protein in a cohort of serous ovarian carcinomas and cell lines. In the presnet study, the expression of PTCH1 protein in the tumor epithelium, connective stroma and whole tissue sections of serous ovarian carcinomas and the healthy epithelium, stroma and whole tissue sections of ovaries and fallopian tubes (controls) was analyzed. Although the exact origin of LGSC and HGSC is still unknown, LGSC most likely arises from FTE (6). Given that the origin of HGSC is probably dual (OSE or FTE) (7), both ovarian and fallopian tube tissues were used as controls in the current study. In addition to tumor epithelium, PTCH1 protein expression was also analyzed in the connective stroma of serous ovarian carcinomas to examine its role in the tumor microenvironment. The connective stroma of the tumor is not tumor tissue, but it may interact with tumor cells and promote tumor growth, proliferation, angiogenesis, invasiveness and metastasis.

The results from the present study showed that total expression of PTCH1 protein was notably higher in the tumor cells of HGSCs and LGSCs compared with OSE and FTE, as well as in HGSC cell lines compared with the control cell line. Increased expression of this protein in serous ovarian carcinomas suggests its active involvement in the pathogenesis of these cancers, consistent with previous studies where increased expression of the PTCH1 protein was associated with tumor development (28-32). In this case, PTCH1 protein has a tumor promoter rather than a tumor suppressor role. It should be noted that a significant proportion of serous ovarian carcinomas exhibited nuclear PTCH1 protein expression in cancer cells in the present study. This was further confirmed in HGSC cell lines. Given the lack of information on nuclear PTCH1 expression in the current literature, the specificity of PTCH1 nuclear localization was further explored by IHC on HGSC and LGSC tissue samples and IF on HGSC cell

lines, using four different anti-PTCH1 antibodies. Increased nuclear expression of PTCH1 protein in serous ovarian carcinoma tissues and cell lines was confirmed with all four used antibodies, with only the anti-PTCH1d antibody exhibiting a lower PTCH1 expression. The observed discrepancies in the antibody sensitivity may be due to the differences in their clonality (monoclonal vs. polyclonal) and the epitopes to which they bind (anti-PTCH1d is the only one that binds to a more distant epitope of the PTCH1 antigen) (41). Polyclonal antibodies recognize the cytoplasmic NTD, whereas the monoclonal antibody recognizes the extracellular ECD1 domain of PTCH1 protein.

To examine the subcellular localization of PTCH1 in more detail, the presence of PTCH1 protein in different cellular compartments of HGSC cell lines was analyzed by western blotting using the four aforementioned antibodies. PTCH1 protein was mostly present in the membrane and nuclear soluble fractions when polyclonal antibodies were used. By contrast, in the case of the monoclonal antibody, this protein was mostly present in the cytoplasmic fraction, which is in line with the IF results. Although the western blot results indicated the presence of PTCH1 protein in the membrane fraction (in the case of all four anti-PTCH1 antibodies used in this study), IF analysis suggested that this protein was not present at the plasma membrane. In addition to the membrane, PTCH1 protein may also be present in the endosomes (membrane vesicles) located in the cytoplasm (42). We hypothesize that punctate signals observed in the cytoplasm may represent endosomes with PTCH1 protein that are extracted within the membrane fraction. IF analysis shows the main distribution of the protein, which can be limited by the resolution, antibody efficiency or epitope masking. In the case of western blotting, the membrane fraction was enriched. This fraction can contain any intracellular membranes, such as the endoplasmic reticulum, mitochondria, endosomes and Golgi apparatus, where the protein can be transiently localized. This provides an additional evidence that PTCH1 potentially can be associated with membranes and can be found in different compartments. Notably, fragments of PTCH1 protein of different molecular weights were detected by western blotting with all four antibodies, which indicates the possibility of proteolytic cleavage of this protein and posttranslational modifications of the resulting fragments. Although anti-PTCH1a/c and anti-PTCH1b antibodies recognize the same epitope of the PTCH1 antigen, it is not clear why they showed a different pattern of PTCH1 fragments in the same samples. There is a possibility that different binding affinity to the same epitope result in the observed differences. In addition, divergence between different batches of antibodies can be observed, even though the antibodies have the same catalogue number. N-terminal cytoplasmic fragments (NTFs; not recognized by the anti-PTCH1d monoclonal antibody), may possibly translocate to the nucleus after proteolytic cleavage, thereby performing a hitherto unknown function. At the same time, most of the protein remains in the cytoplasm. Since nuclear expression of PTCH1 was observed in HGSCs, LGSCs and HGSC cell lines, we hypothesize that NTFs most likely modulate the transcriptional activity of cancer driver genes (namely genes that regulate cell proliferation, survival or angiogenesis), which may represent a potential oncogenic mechanism of this protein in serous ovarian carcinoma cells.

Since nuclear localization of PTCH1 protein was also observed in healthy ovarian/fallopian tube tissues and the FNE1 cell line, there is a possibility that N-cleavage of the PTCH1 protein and its translocation into the nucleus is a process that can take place in healthy ovarian cells as well; however, this process may be more common in cancer cells, since nuclear expression of PTCH1 protein was higher in cancer compared with the healthy cells.

Translocation of cytoplasmic domain fragments of transmembrane proteins to the nucleus has already been recognized as a mechanism of direct signaling between these two cellular compartments (43,44) and described in the case of PTCH1 protein (45). Kagawa *et al* (45) showed that PTCH1 protein was subjected to proteolytic cleavage at the C-terminus, resulting in the generation of a soluble C-terminal fragment, ICD7. They observed that ICD7 fragments accumulate in the cell nucleus of HeLa cells stably expressing full-length PTCH1, where they modulate the transcriptional activity of the GLI1 protein. At the same time, the N-terminal region remained in the cytoplasmic punctates, which may correspond to multivesicular bodies and endosomes, and did not translocate to the nucleus. In addition, nuclear accumulation of endogenous PTCH1 ICD7 fragments was also observed in mouse embryonic fibroblasts (C3H10T1/2 cells) and mouse embryonic primary cells (45). Although Kagawa *et al* (45) also found that these fragments have certain regulatory roles, their biological importance remains unknown. However, the results of the present study indicated the possibility of proteolytic cleavage of the PTCH1 N-terminal cytoplasmic region, resulting in the generation of soluble NTFs that are translocated to the nucleus. To the best of our knowledge, this is the first study to indicate the presence of NTFs of the PTCH1 protein in the nucleus. Since nuclear localization of these fragments was detected in serous ovarian carcinoma cells, we hypothesize that they could play an active tumor promoter role in the nucleus of these malignant cells. This process is still unknown, therefore further studies are required to clarify the role of NTFs in the nucleus of both healthy and cancer cells.

Since PTCH1 protein and gene expression may be affected by epigenetic changes, such as DNA methylation (25-27), the methylation status of the *PTCH1* gene was also analyzed. DNA promoter methylation of *PTCH1* was exclusively found in HGSCs (13.5%). However, *PTCH1* gene promoter methylation did not affect the PTCH1 protein expression in HGSCs. Notably, DNA promoter methylation of the *PTCH1* gene has been previously observed in benign ovarian tumors, such as ovarian dermoids and fibromas (46), but not in ovarian carcinomas (47).

The present data indicated that PTCH1 protein may be actively involved in the pathogenesis of serous ovarian carcinomas. The current study reported the nuclear localization of PTCH1 protein in serous ovarian cells for the first time, to the best of our knowledge. Since the results depended on the specificity of the antibodies used, this may represent a potential limitation of the present study. To overcome this limitation, expression of an N-terminally-tagged (such as FLAG or T7) version of PTCH1 protein in the cell lines would allow independent verification of NTFs in the nucleus. Nevertheless, the punctate signals in the cytoplasm require

further investigation. The membrane-associated fractions of PTCH1 could correspond to an internalized pool of PTCH1 protein, which follows the endosomal pathway either to be recycled back to the plasma membrane or to be degraded by the lysosomal pathway. Further co-localization assays using compartment-specific markers or electron microscopy analysis should be carried out to determine the exact localization of PTCH1 protein. *PTCH1* gene promoter methylation was exclusively observed in HGSC. Further studies are necessary to depict other genomic (such as mutations) and epigenetic (such as histone modifications) alterations of *PTCH1* that may contribute to its activation.

### Acknowledgements

The authors would like to thank Professor Ivan Đikić (Institute of Biochemistry II, School of Medicine, Goethe University, 60590 Frankfurt am Main, Germany) for permitting conduction of part of the present study in his laboratory, which has significantly contributed to the realization of this research.

### Funding

This research was co-financed by the European Union through the Europe Regional Development Fund, Operational Programme Competitiveness and Cohesion (grant no. KK.01.1.1.01.0008; Reproductive and Regenerative Medicine-Exploring New Platforms and Potentials).

### Availability of data and materials

The datasets used and/or analyzed during the current study are available from the corresponding author on reasonable request.

### Authors' contributions

VKK contributed to conceptualization, interpretation, data acquisition and analysis, performed experimental work, wrote and edited the manuscript, and revised the manuscript for important intellectual content. ACP contributed to conceptualization, interpretation and design of the experiments, and revised the manuscript for important intellectual content. AS contributed to data analysis and interpretation, and revised the manuscript for important intellectual content. SV contributed to data analysis and interpretation, and revised the manuscript for important intellectual content. LS conceived the idea of the present study, contributed to conceptualization, data collection and analysis and interpretation of the results, and revised the manuscript for important intellectual content. VKK and LS confirm the authenticity of all the raw data. All authors read and approved the final manuscript.

### Ethics approval and consent to participate

The study was conducted according to the guidelines of the Declaration of Helsinki and approved by the Ethical Committee of School of Medicine, University of Zagreb (approval no. 380-59-10106-20-111/130; 7th October 2020; Zagreb, Croatia) and the Ethical Committee of University Hospital

Merkur Zagreb (approval no. 03/1-11080; 7th December 2017; Zagreb, Croatia; approval no. 30/1-11088; 7th December 2017; Zagreb, Croatia). Written informed consent was obtained from all participants involved in the study.

### Patient consent for publication

Not applicable.

### Competing interests

The authors declare that they have no competing interests.

### References

1. Bray F, Ferlay J, Soerjomataram I, Siegel RL, Torre LA and Jemal A: Global cancer statistics 2018: GLOBOCAN estimates of incidence and mortality worldwide for 36 cancers in 185 countries. *CA Cancer J Clin* 68: 394-424, 2018.
2. Jacobs IJ and Menon U: Progress and challenges in screening for early detection of ovarian cancer. *Mol Cell Proteomics* 3: 355-366, 2004.
3. Ebell MH, Culp MB and Radke TJ: A systematic review of symptoms for the diagnosis of ovarian cancer. *Am J Prev Med* 50: 384-394, 2016.
4. Matulonis UA, Sood AK, Fallowfield L, Howitt BE, Sehouli J and Karlan BY: Ovarian cancer. *Nat Rev Dis Primers* 2: 16061, 2016.
5. Prat J, D'Angelo E and Espinosa I: Ovarian carcinomas: At least five different diseases with distinct histological features and molecular genetics. *Hum Pathol* 80: 11-27, 2018.
6. Wang Y, Hong S, Mu J, Wang Y, Lea J, Kong B and Zheng W: Tubal origin of 'ovarian' low-grade serous carcinoma: A gene expression profile study. *J Oncol* 2019: 8659754, 2019.
7. Hao D, Li J, Jia S, Meng Y, Zhang C, Wang L and Di LJ: Integrated analysis reveals tubal- and ovarian-originated serous ovarian cancer and predicts differential therapeutic responses. *Clin Cancer Res* 23: 7400-7411, 2017.
8. Kotsopoulos IC, Papanikolaou A, Lambropoulos AF, Papazisis KT, Tsolakidis D, Touplikioti P and Tarlatzis BC: Serous ovarian cancer signaling pathways. *Int J Gynecol Cancer* 24: 410-417, 2014.
9. Chen Q, Gao G and Luo S: Hedgehog signaling pathway and ovarian cancer. *Chin J Cancer Res* 25: 346-353, 2013.
10. Szkandera J, Kiesslich T, Haybaeck J, Gerger A and Pichler M: Hedgehog signaling pathway in ovarian cancer. *Int J Mol Sci* 14: 1179-1196, 2013.
11. Jeng KS, Chang CF and Lin SS: Sonic hedgehog signaling in organogenesis, tumors, and tumor microenvironments. *Int J Mol Sci* 21: 758, 2020.
12. Skoda AM, Simovic D, Karin V, Kardum V, Vranic S and Serman L: The role of the hedgehog signaling pathway in cancer: A comprehensive review. *Bosn J Basic Med Sci* 18: 8-20, 2018.
13. Ryan KE and Chiang C: Hedgehog secretion and signal transduction in vertebrates. *J Biol Chem* 287: 17905-17913, 2012.
14. Hanna A and Shevde LA: Hedgehog signaling: Modulation of cancer properties and tumor microenvironment. *Mol Cancer* 15: 24, 2016.
15. Guo YY, Zhang JY, Li XF, Luo HY, Chen F and Li TJ: PTCH1 gene mutations in keratocystic odontogenic tumors: A study of 43 Chinese patients and a systematic review. *PLoS One* 8: e77305, 2013.
16. Rudolf AF, Kinnebrew M, Kowatsch C, Ansell TB, El Omari K, Bishop B, Pardon E, Schwab RA, Malinauskas T, Qian M, *et al*: The morphogen Sonic hedgehog inhibits its receptor patched by a pincer grasp mechanism. *Nat Chem Biol* 15: 975-982, 2019.
17. Fleet AJ and Hamel PA: The protein-specific activities of the transmembrane modules of Ptc1 and Ptc2 are determined by their adjacent protein domains. *J Biol Chem* 293: 16583-16595, 2018.
18. Riobo-Del Galdo NA, Lara Montero Á and Wertheimer EV: Role of hedgehog signaling in breast cancer: Pathogenesis and therapeutics. *Cells* 8: 375, 2019.

19. Shimokawa T, Svärd J, Heby-Henricson K, Teglund S, Toftgård R and Zaphiropoulos PG: Distinct roles of first exon variants of the tumor-suppressor patched1 in hedgehog signaling. *Oncogene* 26: 4889-4896, 2007.
20. Wils LJ and Bijlsma MF: Epigenetic regulation of the hedgehog and Wnt pathways in cancer. *Crit Rev Oncol Hematol* 121: 23-44, 2018.
21. Chung JH and Bunz F: A loss-of-function mutation in PTCH1 suggests a role for autocrine hedgehog signaling in colorectal tumorigenesis. *Oncotarget* 4: 2208-2211, 2013.
22. Wang CY, Chang YC, Kuo YL, Lee KT, Chen PS, Cheung CHA, Chang CP, Phan NN, Shen MR and Hsu HP: Mutation of the PTCH1 gene predicts recurrence of breast cancer. *Sci Rep* 9: 16359, 2019.
23. Musani V, Sabol M, Car D, Ozretic P, Oreskovic S, Leovic D and Levanat S: LOH of PTCH1 region in BCC and ovarian carcinoma: Microsatellite vs HRM analysis. *Front Biosci (Elite Ed)* 4: 1049-1057, 2012.
24. McGarvey TW, Maruta Y, Tomaszewski JE, Linnenbach AJ and Malkowicz SB: PTCH gene mutations in invasive transitional cell carcinoma of the bladder. *Oncogene* 17: 1167-1172, 1998.
25. Heitzer E, Bambach I, Dandachi N, Horn M and Wolf P: PTCH promoter methylation at low level in sporadic basal cell carcinoma analysed by three different approaches. *Exp Dermatol* 19: 926-928, 2010.
26. Sinha S, Singh RK, Alam N, Roy A, Roychoudhury S and Panda CK: Alterations in candidate genes PHF2, FANCC, PTCH1 and XPA at chromosomal 9q22.3 region: Pathological significance in early- and late-onset breast carcinoma. *Mol Cancer* 7: 84, 2008.
27. Zuo Y, Song Y, Zhang M, Xu Z and Qian X: Role of PTCH1 gene methylation in gastric carcinogenesis. *Oncol Lett* 8: 679-682, 2014.
28. Im S, Choi HJ, Yoo C, Jung JH, Jeon YW, Suh YJ and Kang CS: Hedgehog related protein expression in breast cancer: gli-2 is associated with poor overall survival. *Korean J Pathol* 47: 116-123, 2013.
29. Gonnissen A, Isebaert S, Perneel C, McKee CM, Van Utterbeeck F, Lerut E, Verrill C, Bryant RJ, Joniau S, Muschel RJ and Haustermans K: Patched 1 expression correlates with biochemical relapse in high-risk prostate cancer patients. *Am J Pathol* 188: 795-804, 2018.
30. Hasanovic A and Mus-Veteau I: Targeting the multidrug transporter Pchl1 potentiates chemotherapy efficiency. *Cells* 7: 107, 2018.
31. Chen X, Horiuchi A, Kikuchi N, Osada R, Yoshida J, Shiozawa T and Konishi I: Hedgehog signal pathway is activated in ovarian carcinomas, correlating with cell proliferation: It's inhibition leads to growth suppression and apoptosis. *Cancer Sci* 98: 68-76, 2007.
32. Liao X, Siu MK, Au CW, Wong ES, Chan HY, Ip PP, Ngan HY and Cheung AN: Aberrant activation of hedgehog signaling pathway in ovarian cancers: Effect on prognosis, cell invasion and differentiation. *Carcinogenesis* 30: 131-140, 2009.
33. Bhattacharya R, Kwon J, Ali B, Wang E, Patra S, Shridhar V and Mukherjee P: Role of hedgehog signaling in ovarian cancer. *Clin Cancer Res* 14: 7659-7666, 2008.
34. Zheng F, Xiao X and Wang C: The effect of PTCH1 on ovarian cancer cell proliferation and apoptosis. *Cancer Biother Radiopharm* 34: 103-109, 2019.
35. Kardum V, Karin V, Glibo M, Skrtic A, Martic TN, Ibisevic N, Skenderi F, Vranic S and Serman L: Methylation-associated silencing of SFRP1 gene in high-grade serous ovarian carcinomas. *Ann Diagn Pathol* 31: 45-49, 2017.
36. Karin-Kujundzic V, Kardum V, Sola IM, Paic F, Skrtic A, Skenderi F, Serman A, Nikuseva-Martic T, Vranic S and Serman L: Dishevelled family proteins in serous ovarian carcinomas: A clinicopathologic and molecular study. *APMIS* 128: 201-210, 2020.
37. Vrsalovic MM, Korac P, Dominis M, Ostojic S, Mannhalter C and Kusec R: T- and B-cell clonality and frequency of human herpes viruses-6, -8 and Epstein Barr virus in angioimmunoblastic T-cell lymphoma. *Hematol Oncol* 22: 169-177, 2004.
38. Peng L, Hu J, Li S, Wang Z, Xia B, Jiang B, Li B, Zhang Y, Wang J and Wang X: Aberrant methylation of the PTCH1 gene promoter region in aberrant crypt foci. *Int J Cancer* 132: E18-E25, 2013.
39. McDonald D, Carrero G, Andrin C, de Vries G and Hendzel MJ: Nucleoplasmic beta-actin exists in a dynamic equilibrium between low-mobility polymeric species and rapidly diffusing populations. *J Cell Biol* 172: 541-552, 2006.
40. Hooek TC, Newcomb PM and Herman IM: Beta actin and its mRNA are localized at the plasma membrane and the regions of moving cytoplasm during the cellular response to injury. *J Cell Biol* 112: 653-664, 1991.
41. Acharya P, Quinlan A and Neumeister V: The ABCs of finding a good antibody: How to find a good antibody, validate it, and publish meaningful data. *FI000Res* 6: 851, 2017.
42. Pak E and Segal RA: Hedgehog signal transduction: Key players, oncogenic drivers, and cancer therapy. *Dev Cell* 38: 333-344, 2016.
43. Carpenter G: Nuclear localization and possible functions of receptor tyrosine kinases. *Curr Opin Cell Biol* 15: 143-148, 2003.
44. Anido J, Scaltriti M, Bech Serra JJ, Santiago Josef B, Todo FR, Baselga J and Arribas J: Biosynthesis of tumorigenic HER2 C-terminal fragments by alternative initiation of translation. *EMBO J* 25: 3234-3244, 2006.
45. Kagawa H, Shino Y, Kobayashi D, Demizu S, Shimada M, Ariga H and Kawahara H: A novel signaling pathway mediated by the nuclear targeting of C-terminal fragments of mammalian patched 1. *PLoS One* 6: e18638, 2011.
46. Cretnik M, Musani V, Oreskovic S, Leovic D and Levanat S: The patched gene is epigenetically regulated in ovarian dermoids and fibromas, but not in basocellular carcinomas. *Int J Mol Med* 19: 875-883, 2007.
47. Löf-Öhlin ZM, Levanat S, Sabol M, Sorbe B and Nilsson TK: Promoter methylation in the PTCH gene in cervical epithelial cancer and ovarian cancer tissue as studied by eight novel Pyrosequencing® assays. *Int J Oncol* 38: 685-692, 2011.



This work is licensed under a Creative Commons Attribution-NonCommercial-NoDerivatives 4.0 International (CC BY-NC-ND 4.0) License.